Neuropsychopharmacology (2015) 40, 1259–1268

www.neuropsychopharmacology.org

The Neurometabolic Fingerprint of Excessive Alcohol Drinking

Marcus W Meinhardt*[,1,5], Daniel C Sévin[2,3,5], Manuela L Klee[1], Sandra Dieter[1], Uwe Sauer[2] and Wolfgang H Sommer[1,4]

[1]Institute of Psychopharmacology at Central Institute of Mental Health, Medical Faculty Mannheim, University of Heidelberg, Mannheim, Germany; [2]Institute of Molecular Systems Biology, ETH Zürich, Zürich, Switzerland; [3]PhD Program on Systems Biology, Life Science Zurich, Zurich, Switzerland; [4]Department of Addiction Medicine at Central Institute of Mental Health, Medical Faculty Mannheim, University of Heidelberg, Mannheim, Germany

'Omics' techniques are widely used to identify novel mechanisms underlying brain function and pathology. Here we applied a novel metabolomics approach to further ascertain the role of frontostriatal brain regions for the expression of addiction-like behaviors in rat models of alcoholism. Rats were made alcohol dependent via chronic intermittent alcohol vapor exposure. Following a 3-week abstinence period, rats had continuous access to alcohol in a two-bottle, free-choice paradigm for 7 weeks. Nontargeted flow injection time-of-flight mass spectrometry was used to assess global metabolic profiles of two cortical (prelimbic and infralimbic) and two striatal (accumbens core and shell) brain regions. Alcohol consumption produces pronounced global effects on neurometabolomic profiles leading to a clear separation of metabolic phenotypes between treatment groups, particularly. Further comparisons of regional tissue levels of various metabolites, most notably dopamine and Met-enkephalin, allow the extrapolation of alcohol consumption history. Finally, a high-drinking metabolic fingerprint was identified indicating a distinct alteration of central energy metabolism in the accumbens shell of excessively drinking rats that could indicate a so far unrecognized pathophysiological mechanism in alcohol addiction. In conclusion, global metabolic profiling from distinct brain regions by mass spectrometry identifies profiles reflective of an animal's drinking history and provides a versatile tool to further investigate pathophysiological mechanisms in alcohol dependence.
Neuropsychopharmacology (2015) **40,** 1259–1268; doi:10.1038/npp.2014.312; published online 17 December 2014

INTRODUCTION

Excessive alcohol consumption is one of the biggest public health concerns in most developed countries. In the European Community alone, which is the biggest market in the world and also one of the heaviest drinking region, nearly 60 million citizens engage in harmful drinking and 23 million Europeans are estimated to suffer from alcohol addiction (Rehm *et al*, 2009). Thus, alcohol use disorders are probably the most prevalent neuropsychiatric disorder afflicting western society today. Many preclinical and human neuroimaging studies suggest a critical involvement of prefrontal–striatal connectivity in the transition to addictive behavior (Spanagel, 2009; Koob and Volkow, 2010). Thus, detailed investigations of the molecular consequences that occur during the transition into addictive behavior are needed for better understanding of underlying mechanisms. For the identification of molecular alterations a widely applied strategy is the use of so-called 'omics' technologies.

The term 'omics' describes a set of methods that enable unbiased simultaneous assessments of thousands of molecular species (ie, genes, transcripts, proteins, or metabolites) in cells, tissues, or organs. In combination with advanced bioinformatics, these methods aim at the systematic and comprehensive analysis of the global profiles and their responses to disease, drug, or other challenges. In brain research, the most common omics approach so far has been transcriptome profiling in animal models or human postmortem brain samples. These studies have led to new mechanistic insights and novel candidate genes for disease mechanisms, but when applied to psychiatric disorders the discriminative power of brain transcriptome profiles to separate cases and controls has typically been low (Reimers *et al*, 2005). We and others have used this approach to identify sustained gene expression patterns in the corticostriatal circuitry induced by chronic alcohol exposure, consumption, and dependence (Mayfield *et al*, 2002; Rimondini *et al*, 2002; Arlinde *et al*, 2004; Sommer *et al*, 2005; Liu *et al*, 2006; Meinhardt *et al*, 2013). Generally, these experiments resulted in interesting and verifiable candidate genes, but could not demonstrate robust discrimination of cases and controls based on their global gene expression profiles.

*Correspondence: Dr MW Meinhardt, Central Institute of Mental Health, University of Heidelberg, Square J5, 68159 Mannheim, Germany, Tel: +49 621 1703 6286, Fax: +49 621 1703 6255, E-mail: marcus.meinhardt@zi-mannheim.de
[5]These authors contributed equally to this work.
Received 8 August 2014; revised 28 October 2014; accepted 13 November 2014; accepted article preview online 24 November 2014

Compared with the transcriptome, the diversity of metabolites, which are the by-products and end-products of synthetic and catabolic pathways within a biological system, appears much closer to the molecular phenotype. Thus, studying metabolic responses complements existing omics techniques in the field and might have more predictive power in identifying phenotypic alterations, as they are more directly linked to the mechanisms involved in the expression of a distinct phenotype than transcript abundances (Dettmer *et al*, 2007; Pasikanti *et al*, 2008; Kaddurah-Daouk and Krishnan, 2009). Recent developments in both analytical platforms and bioinformatics methods now make it possible to define metabolic profiles for diseases of the central nervous system (Yao and Reddy, 2005; Bogdanov *et al*, 2008; Gika *et al*, 2012). Nontargeted mass spectrometry-based metabolomics, in particular, allows the assessment of global neurometabolic profiles in specific brain regions with high selectivity and sensitivity, and thus provides a technique to search for novel pathophysiological mechanisms in alcohol dependence (Patti *et al*, 2012; Sévin and Sauer, 2014).

Here, we tested the hypothesis of whether or not a history of high or low alcohol intake manifests itself in discernible neurometabolic patterns within key regions of the motivation and addiction circuitry (Noori *et al*, 2012). We have previously demonstrated that rats made alcohol dependent by chronic intermittent exposure (CIE) to alcohol vapor develop a stable phenotype of high alcohol consumption (Rimondini *et al*, 2002, 2003; Sommer *et al*, 2008; Meinhardt and Sommer, 2014). After 7 weeks of voluntary access to alcohol, high-drinking and low-drinking rats went through a brief period of alcohol abstinence before brains were harvested and compared by mass spectrometric analysis for their metabolic profiles in prefrontal cortex and nucleus accumbens. We found robust neurometabolic fingerprints in the infralimbic–accumbens shell circuitry that reflect the animal's alcohol-drinking history. Furthermore, alterations in energy metabolism within the nucleus accumbens shell emerge as a new potential mechanism for the pathophysiology of alcohol.

MATERIALS AND METHODS

Animal Husbandry

Male Wistar rats with an initial weight of 220–250 g were used (Charles River, Germany), housed four per cage under a 12 h light/dark cycle with *ad libitum* access to food and water. All experiments were conducted in accordance with the ethical guidelines for the care and use of laboratory animals, and were approved by the local animal care committee (Regierungspraesidium Karlsruhe, Germany).

Ethanol Exposure

Rats were weight matched, assigned into the two experimental groups, and exposed to either ethanol vapor or normal air using a rodent alcohol inhalation system as described previously (Rimondini *et al*, 2002). Briefly, pumps (Ismatec, Wertheim, Germany) delivered alcohol into electrically heated stainless steel coils (72 °C) connected to an airflow of 18 L/min into glass/steel chambers ($1 \times 1 \times 1$ m). For the next 7 weeks, rats were exposed to five cycles of 14 h of ethanol vapor per week (0000 h to 1400 h) separated by daily 10 h periods of withdrawal. Twice per week, blood ($\sim 20\,\mu$L) was sampled from the lateral tail vein and blood alcohol concentrations were determined using an AM1 Analox system (Analox Instruments, London, UK). After the last exposure cycle, rats remained abstinent for 3 weeks before access to alcohol bottles.

Measurement of Ethanol Withdrawal Signs

Using a withdrawal rating scale according to Macey *et al* (1996), alcohol withdrawal signs including irritability to touch (Vocalization), body tremors, tail rigidity, abnormal gait, and ventromedial limb retraction were scored weekly, 6 h after ethanol vapor was turned off. Each sign was assigned a score of 0–2, based on the following severity scale: 0 = no sign, 1 = moderate, and 2 = severe. The sum of the 4 observation scores (0 to 8) was used as a quantitative measure of withdrawal severity. For these behavioral observations, animals were individually transferred from their home cages to a quiet observation room to avoid extraneous stimulation and animals were observed in a blinded manner.

Two-Bottle Free-Choice Paradigm

At 3 weeks after chronic ethanol exposure procedure, ethanol was made continuously available in a two-bottle, free-choice paradigm for 7 weeks. Ethanol concentration was gradually increased over 10 days from 2 to 4% and finally to 8% (v/v). Tap water was continuously available in the second bottle. Ethanol and water intake were measured on Monday, Wednesday, and Friday at the same time and bottle positions were alternated randomly to avoid side preferences. These weights were converted into volumes of solutions, preference of ethanol, and g of ethanol consumed per kg of body weight per day using the specific density of ethanol (0.79). The formula for ethanol intake was (consumed ethanol × percentage of the given ethanol × specific density of ethanol)/body weight × 1000.

Rat Brain Tissue Samples

At 72 h after last access to alcohol bottles, postdependent (alcohol exposed, $n = 11$) and control (air exposed, $n = 11$) animals were killed during the first 4 h of the light cycle by decapitation, and brains were quickly frozen in -40 °C isopentane and kept at -80 °C. Bilateral samples were obtained under a magnifying lens using anatomical landmarks from Paxinos and Watson (1998). Then, 150 μm cryosections of the prelimbic, infralimbic, nucleus accumbens core, and shell were dissected out using a macropunch (2 mm diameter). Samples were stored at -80 °C until extraction. To extract metabolites, 10 mg of macropunches were extracted with 1 mL of preheated 70% (v/v) ethanol/water solution for 2 min at 80 °C with occasional vortexing. After centrifugation for 10 min at 0 °C and 20 800 *g*, supernatants of the extraction solutions were evaporated to dryness under vacuum and pellets were resuspended in 40 μL H_2O and stored at -80 °C before mass spectrometry.

Nontargeted Mass Spectrometry

The mass spectrometric analysis was performed on a platform consisting of a Hitachi L-7100 liquid chromatography pump coupled to a Gerstel MPS2 auto sampler and an Agilent 6550 IonFunnel QTOF (Agilent, Santa Clara, CA) operated with published settings in negative ionization mode (Fuhrer *et al*, 2011) using automated isocratic flow injection without prior chromatographic separation. The flow rate was 150 μL/min of mobile phase consisting of isopropanol/water (60 : 40, v/v) buffered with 5 mM ammonium fluoride at pH 9. For online mass axis correction, 2-propanol (in the mobile phase), taurocholic acid, and hexakis (1H, 1H, 3H-tetrafluoropropoxy)phosphazine (HP-0921, Agilent Technologies) were added to the mobile phase. All samples were measured in technical duplicates. Mass spectra were recorded in profile mode from *m/z* 50 to 1000 with a scan rate of 1.4 spectra/s for 0.48 min using the highest resolving power (4 GHz HiRes). Electrospray source temperature was set to 325 °C, with 5 L/min drying gas and a nebulizer pressure of 30 psig. Spectral processing (profile alignment, peak detection, centroiding, merging) was performed as published previously (Fuhrer *et al*, 2011). All steps of data processing and analysis were performed with Matlab R2013b (The Mathworks, Natick, MA) using functions embedded in the Bioinformatics, Statistics, Database, and Parallel Computing toolboxes (Fuhrer *et al*, 2011). Ions were annotated within 0.001 Da deviation from the theoretical mass of compounds in the Kyoto Encyclopedia of Genes and Genomes (KEGG) *Rattus norvegicus* metabolite database (Kanehisa, 2002), assuming deprotonation $[M-H]^-$ or fluoride addition $[M+F]^-$ and zero or one $^{12}C->^{13}C$ exchange as possible electrospray-derived species.

Statistics and Computational Methods

Alcohol drinking data were analyzed with one-way ANOVA. The withdrawal scores were compared using the Mann–Whitney test. Statistical significance was set at $p<0.05$. Statistica10.0, Software for Windows was used (StatSoft, Tulsa, OK). All subsequent statistical analyses were carried out using Matlab R2013b (The Mathworks) and functions embedded in the Bioinformatics and Statistics toolboxes. Metabolites underwent an unpaired-sample *t*-test assuming unequal variance to test the null hypothesis that the ion intensity is the same in animals with elevated alcohol consumption compared with the low drinkers. *P*-values were corrected for multiple hypothesis testing by adjusting the false discovery rate using the method of Storey and Tibshirani (2003). In the infralimbic and the accumbens shell, 116 metabolite ions passed a false discovery rate (*q*-value) cutoff of 0.05 and were thus considered as significantly altered. Principal component analysis (PCA) was performed based on annotated ion intensities, and resulting cluster separation was assessed according to 95% confidence intervals calculated using χ^2 tests. Correlation of metabolite ion intensity with animal alcohol intake using a linear model was assessed by Pearson's correlation coefficient (R^2) and tested for statistical significance ($p<0.05$, χ^2 test), and the goodness of fit of a Heaviside-type step model to these data was assessed by the total sum of squared residuals. Metabolic pathway enrichment analysis was performed based on metabolites in respective clusters using the KEGG *R. norvegicus* metabolic pathway definitions (Kanehisa, 2002), and statistical significance of enrichments was assessed using hypergeometric tests. Hierarchical clustering based on metabolite ion correlations or enriched pathways was performed using the Euclidean distance metric.

RESULTS

Compared with nonexposed controls, chronic intermittent exposure of rats to alcohol vapor for 7 weeks resulted in significant signs of withdrawal after discontinuation of alcohol ($\sim$4 out of maximal 8 points from a global withdrawal score (Macey *et al*, 1996); $p<0.001$; Mann–Whitney *U*-test, Figure 1a). Following 3 weeks of abstinence, both postdependent and control rats ($n=11$/group) were given access to tap water and 8% (v/v) alcohol solution in a two-bottle free-choice paradigm for 7 weeks. As previously shown (Rimondini *et al*, 2002), postdependent rats consumed significantly increased amounts of alcohol (total mean intake over time: control 0.92 g/kg/day; postdependent 2.64 g/kg/day; $p<0.001$; one-way ANOVA, Figure 1b). Notably, within each group, two rats displayed a markedly different drinking behavior that exceeded 1 SD range, that is, low-drinking postdependent or high-drinking control rats (Figure 1b). Brains were collected 3 days after the last alcohol access to avoid potential interference from acute withdrawal.

Subsequently, metabolites were extracted from brain region tissues and their levels were measured using nontargeted flow injection time-of-flight mass spectrometry (Fuhrer *et al*, 2011). Out of 10 593 detected *m/z* features (ions), 2126 could be annotated by accurate mass, corresponding to up to 2155 unique metabolites using compounds in the KEGG (see Kanehisa, 2002) *R. norvegicus* database as reference (Supplementary Table 1).

PCA was used to identify major sources of variance in the data set from the four sampled brain regions. As shown in Figure 1c, notably the two cortical regions (prelimbic and infralimbic cortex) separated into two distinct clusters on the two-dimensional plane spanned by the first two principal components that explain 95.7% of the variance. The two striatal brain regions (nucleus accumbens core and shell) together separated from the cortical regions, but did not separate from each other. We next asked which metabolites explained most of the data set variance and thus contributed most to the separation of the brain regions along the first two principal components. Intriguingly, the 25 most influencing metabolites included a number of well-known neuroactive compounds, such as *N*-acetylaspartate, glutamate, glutamine, creatinine, γ-aminobutyric acid (GABA), *myo*-inositol, and dopamine (Table 1). In conclusion, the different brain regions, independent of the factor alcohol consumption, show distinct metabolome profiles that characteristically differ in the respective levels of neuroactive compounds.

To investigate whether or not high alcohol consumption itself would be associated with a distinct neurometabolic phenotype, we performed brain region-specific PCAs and separated the data sets along the first two principal

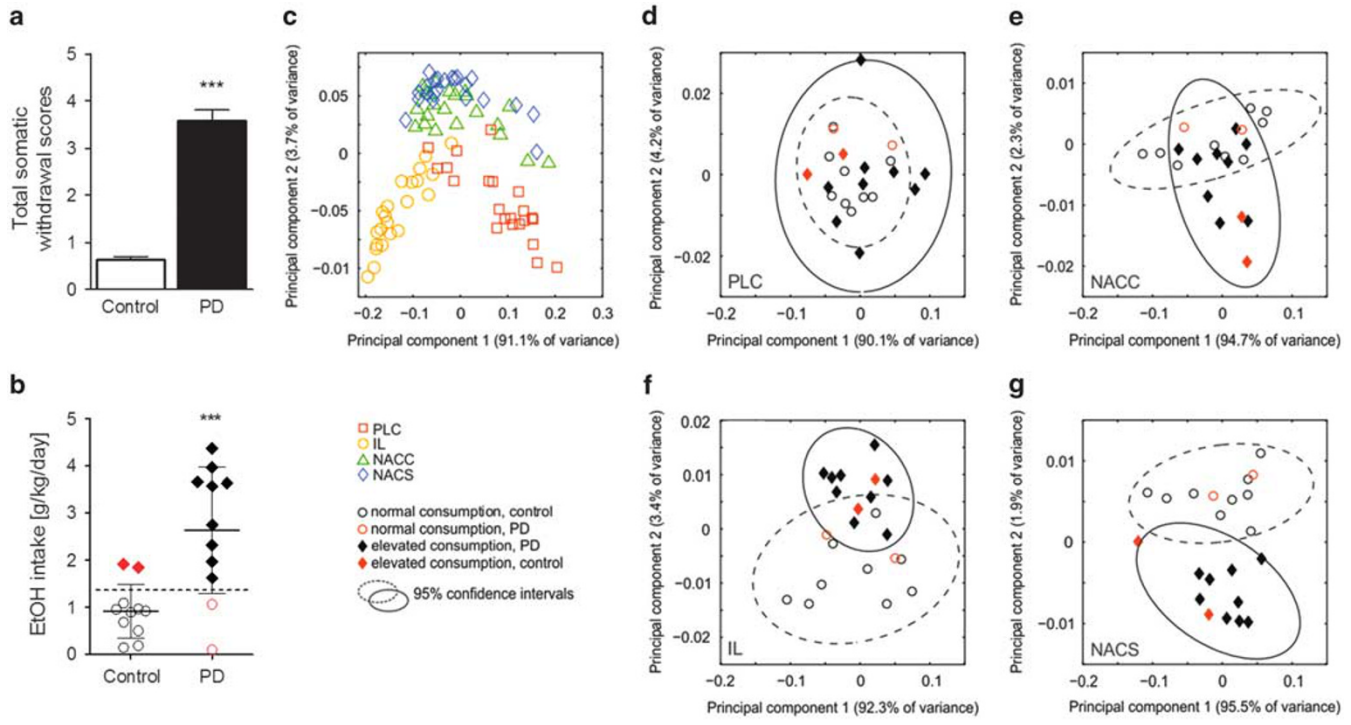

Figure 1 Increased total somatic withdrawal signs and long-lasting excessive alcohol drinking in postdependent rats and principal component analysis of the infralimbic (IL), prelimbic (PLC), accumbens core (NACC), and accumbens shell (NACS) based on annotated metabolite ion levels. (a) After 7 weeks of exposure, withdrawal signs were scored 8 h after last intoxication cycle. Total somatic withdrawal scores consist of the sum of the somatic withdrawal scores across the five behavioral signs of alcohol withdrawal (ventromedial limb retraction, vocalization, tail stiffness, abnormal gait, and body tremors). (b) Following 3 weeks of abstinence, rats had access to either tap water or 8% (v/v) alcohol. Postdependent (PD) rats show higher alcohol consumption than controls. Within the controls, two rats show increased drinking, exceeding the SD range (marked as red hashes). Also within the PD group, two rats consumed very low amounts of alcohol (marked as red circles). (c–g) Displayed are the first two principal components explaining ~97% of the data set variance. Data sets are highlighted based on brain region (c) or alcohol exposure and consumption history of the animals (d–g). (c) The infralimbic cortex (orange circles) and the prelimbic cortex (red squares) have a metabolic phenotype that is distinct from the two nucleus accumbens regions (core: green triangles; shell: blue hashes) that do not separate. The levels of alcohol consumption result in distinct metabolite profiles for the infralimbic (f) and nucleus accumbens shell (g) but not for the prelimbic (d) and nucleus accumbens core (e). Ellipses represent the 95% confidence interval for the consumption classes. ***$P<0.001$.

components. Subsequently, we calculated 95% confidence intervals for the data sets of control and excessively consuming animals. Although no distinct clusters emerged in prelimbic cortex and nucleus accumbens core (Figure 1d and e), we found distinct clusters for the infralimbic region that are partially explained by the alcohol consumption history of the rats (Figure 1f). Strikingly, low- and high-consuming animals almost completely segregated based on their metabolome profiles in the nucleus accumbens shell (Figure 1g) that aligns well with the known role of this region in alcohol reward (Imperato and Di Chiara, 1986; Di Chiara and Imperato, 1988; Pontieri *et al*, 1995; Howland *et al*, 2002; Parsons *et al*, 2007). Our results therefore indicate that excessive alcohol consumption indeed affects neurometabolism in a brain region-specific manner, particularly in the infralimbic–accumbens shell circuit.

Furthermore, PCA suggests that animals appear to segregate according to observed drinking pattern rather than history of dependence, that is, the two low drinkers from the postdependent group cluster closely with the control animals, whereas the two high-drinking control animals cluster with the postdependent group. Consequently, we reassigned the animals into a low-drinking and a high-drinking group (mean daily intake below or above 1.2 g/kg, respectively, $n=11$/group) for analysis of alcohol-responsive metabolites, restricting to the infralimbic and accumbens shell regions because, according to the PCA, neurometabolite levels showed the strongest alcohol-dependent variation in these regions.

Correlation analysis of metabolite ion levels with the average daily alcohol consumption by the animals revealed 246 out of 2155 metabolite ions with significant correlation ($P<0.05$, χ^2 test, uncorrected) in either accumbens shell or infralimbic region (Supplementary Table 2). Highly significant correlations were found for dopamine (IL: $R^2=-0.63$, $p=9.87\text{E}-6$; NACS: $R^2=0.37$, $p=2.61\text{E}-3$) and Met-enkephalin (IL: $R^2=-0.42$, $p=1.03\text{E}-3$; NACS: $R^2=0.20$, $p=3.86\text{E}-2$). Interestingly, levels of these metabolites were increased in the nucleus accumbens shell but decreased in the infralimbic region in high-drinking animals (Figure 2a). Although dopamine levels show a stepwise response, Met-enkephalin levels changed gradually and correlated well with the actual daily alcohol intake.

These metabolite ions significantly correlating with alcohol intake were then hierarchically clustered based on their correlation coefficients (R^2) in the respective brain region using Euclidean distance metric. Ten clusters with distinct correlation patterns were obtained, whereby each

Table 1 Unambiguous and Most Probable Ion *m/z* Values Explaining the Most Influential Compounds of the PCA

Rank	*m/z*	Compounds
1	174.0406	*N*-acetyl-L-aspartate
2	255.2348	Hexadecanoic acid
3	175.0243	L-2,4-diaminobutanoate
4	283.2663	Octadecanoic acid
5	179.0558	*myo*-Inositol
6	145.0614	L-Glutamine
7	124.0068	Taurine
8	146.0455	L-Glutamate
9	134.0465	4-Hydroxy-L-threonine
10	128.0347	4-Oxoproline
11	112.0509	Creatinine
12	306.0765	Glutathione
13	346.0562	*N*-acetylneuraminate
14	303.2347	(9Z)-Octadecenoic acid
15	341.1083	Sucrose
16	242.0798	Cytidine
17	214.0484	*N*-acetyl-L-glutamate 5-semialdehyde
18	152.0713	Dopamine
19	218.1034	Pantothenate
20	265.1481	Tetradecanoic acid
21	256.2375	Hexadecanoic acid
22	167.043	L-Glutamine
23	127.0506	γ-Amino-gamma-cyanobutanoate
24	281.2497	(9Z)-Octadecenoic acid
25	130.0502	L-Glutamate 5-semialdehyde

For the full annotation please see Supplementary Table 1.

cluster contained metabolites with exclusively positive or negative correlation coefficients in one or both brain regions (Figure 2b). For example, cluster 8 contains metabolites that only correlate negatively with alcohol intake in the nucleus accumbens shell but do not show any correlation in the infralimbic cortex. In contrast, cluster 10 metabolites show positive correlation with alcohol intake in the nucleus accumbens shell but negative correlation in the IL, a pattern similar to dopamine and Met-enkephalin as described above. Thus, metabolites sharing a similar physiological response to alcohol consumption across the investigated brain regions can be grouped into distinct clusters, possibly suggesting underlying pathophysiological mechanisms.

To investigate whether metabolites within a cluster are indeed involved in shared physiological processes, we performed a metabolic pathway enrichment analysis. We found 66 pathways that were significantly enriched in at least one cluster (Figure 3; $P<0.05$, hypergeometric test), implying that distinct correlation patterns reflect meaningful physiological effects of metabolically related compounds. Together, clustered metabolite correlations and enriched metabolic pathways thereby provide an overview of how compounds involved in different metabolic processes are generally associated with excessive alcohol intake.

To obtain an even more general view of the alcohol-induced changes in metabolism, we hierarchically clustered the enriched pathways based on the enrichment significance, leading to three independent KEGG categories of broad biological functions (lipid metabolism, central carbon and energy metabolism, addiction, and neurotransmission). Within each group of biological function, a consensus metabolite correlation pattern was then determined by averaging correlations of the individual clusters. These consensus correlation patterns can thus be interpreted as the prototypic metabolic responses of different functional biological groups to elevated alcohol consumption. In this analysis, cluster 8 represents mostly central metabolic pathways, whereas cluster 10 seems more associated with neurotransmission and pathways that are typically afflicted by addictive drugs (Figure 3). The significant enrichment of metabolic pathways in the category of addiction and neurotransmission was particularly intriguing, because it implies that multiple neuroactive compounds share similar cross-brain correlation patterns that might form a metabolic fingerprint characteristic for addiction in general and alcohol dependence in particular.

Another interesting group includes multiple pathways involved in central carbon and energy metabolism. Levels of metabolites involved in these pathways tended to show a negative correlation with alcohol intake in the nucleus accumbens shell (Figure 3, cluster 8). Elevated alcohol consumption has been previously shown to reduce the activity of transketolase (Alexander-Kaufman and Harper, 2009), a key enzyme in the pentose phosphate pathway (PPP) used for the generation of reduced nicotine adenine dinucleotide phosphate (NADPH), a cofactor for many enzymes involved in managing oxidative stress. Indeed, we observed reduced levels of metabolites in the PPP as well as in the upper glycolytic pathway (Figure 4), consistent with an effect of elevated alcohol consumption on cerebral energy metabolism. Furthermore, rats with elevated alcohol consumption accumulate acetyl coenzyme A that can be either secreted as lactate or serve as a precursor for lipid metabolism.

DISCUSSION

This report represents, to our knowledge, the first mass spectrometry-based global metabolic profiling from microdissected tissue samples of brain regions implicated in the pathology of alcoholism. The study generated several interesting new insights: (1) distinct brain regions, even closely related ones such as the infralimbic and prelimbic areas within the rat mPFC, can be separated based on their metabolic phenotypes; (2) alcohol consumption profoundly alters regional neurometabolomic profiles, particularly in brain circuits known to be highly sensitive to long-term effects of alcohol, that is, the infralimbic–accumbens shell circuit (Meinhardt *et al*, 2013); (3) regional tissue concentration of some metabolites, most notably of dopamine and Met-enkephalin, allows the extrapolation of recent drinking history; and (4) the identification of an alcohol-drinking-related metabolic fingerprint that persists beyond the actual drinking period and could indicate a so far unrecognized pathophysiological mechanism in alcohol

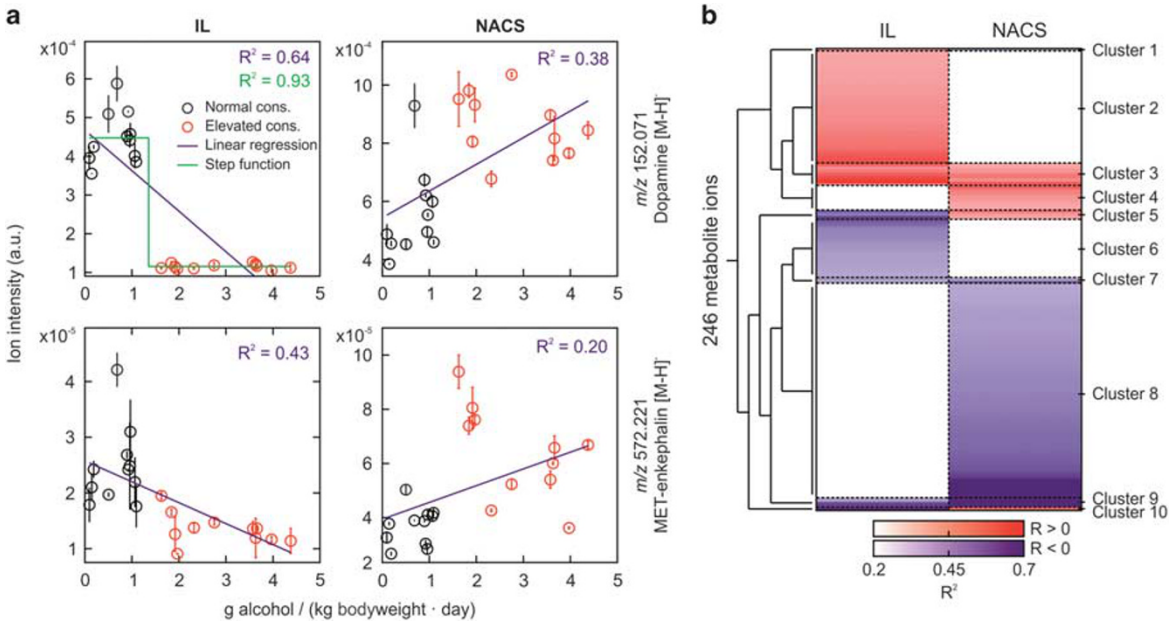

Figure 2 Correlation analysis of dopamine and Met-enkephalin with alcohol intake and hierarchical clustering of 246 ions, based on their correlation with alcohol intake. (a) The brain metabolite levels of dopamine and Met-enkephalin significantly ($p<0.05$, χ^2 test) correlate with the amounts of daily alcohol intake. Within the infralimbic, levels of both metabolite decrease whereas they increase in the accumbens shell. Black points show data from normal-consuming and red points from elevated-consuming rats. Linear regression lines are shown in blue, and step functions in green if $R^2 \geq 0.6$. (b) The intensities of all 2155 metabolite ions in the infralimbic–accumbens shell pathway were correlated with the daily alcohol intake of the animals. A total of 246 ions showed a significant ($p<0.05$, χ^2 test) correlation with alcohol intake in at least one brain region. Red color indicates a positive and blue color a negative correlation with the daily alcohol intake. R^2 is Pearson's correlation coefficient. Ions were clustered by R^2 using the Euclidean distance metric. For details in color coding of each cluster, see top panel in figure 3.

addiction. Together, the study demonstrated that global metabolic profiling by mass spectrometry is a feasible approach for studying the alterations of the metabolome in postmortem brain tissue, and thus comprises a highly useful extension to the arsenal of existing omics technologies used for deciphering the pathology of neuropsychiatric disorders including alcohol addiction.

Using nontargeted mass spectrometry to analyze the neurometabolome is a novel technique that has so far been rarely used on brain tissue (Masuo *et al*, 2009; Deng *et al*, 2012; Zaitsu *et al*, 2013), especially not to discern subregions of the brain. The mass spectrometric method used here allows rapid assessment of the complete metabolome with very high resolution. A drawback of the present method is that some metabolites can share the same mass/charge relation and thus cannot be distinguished. Most ambiguities could be resolved by the fact that many computationally annotated constitutional isomers are not known to be present in brain tissue or even in mammals, justifying curation of the annotations to focus on most relevant metabolites. Nevertheless, interesting candidate ions showing such ambiguities may require further verification by corroborative methods that allow to resolve the molecular structure such as MS/MS or NMR.

The brain samples of this study were derived from two groups of alcohol-drinking animals: one group with a history of high alcohol exposure leading to the development of dependence and excessive consumption of alcohol, and a control group without high-level alcohol exposure that was drinking at baseline levels. Importantly, during nearly 2 months of free alcohol access, two animals from the control group increased their alcohol intake up to the level of the alcohol-dependent group, whereas two exposed rats were resistant to developing high-level drinking. Strikingly, these animals also share similar metabolic profiles with the respective high- or low-drinking animals. Spontaneous development of high alcohol consumption in outbred rodent populations is well known and widely used to breed high alcohol-preferring lines. In fact, such experiments were among the first to establish the heritability of alcohol-drinking phenotypes. However, similar to humans (Treutlein *et al*, 2006; Gelernter *et al*, 2014), individual genetic variants in rodent populations explain only a small proportion of the observed variance in alcohol drinking (Björk *et al*, 2010; Ayanwuyi *et al*, 2013; Zhou *et al*, 2013), and so far it is not possible to make robust predictions about drinking outcomes based on genetic profiling. Given the robust alterations associated with high alcohol consumption observed here, future studies should elucidate whether neurometabolic profiles, at least in part, comprise predisposing factors. This hypothesis is supported by the fact that alcohol does not seem to induce global alterations in all assessed brain regions, but only in a distinct functionally connected circuit. A subsequent question is whether such potential risk profiles are mirrored in easy accessible peripheral tissues to serve as prognostic biomarkers in humans.

Interestingly, dopamine and Met-enkephalin tissue levels in the accumbens shell showed a robust positive correlation to previous levels of alcohol consumption. The association of altered dopamine levels during acute alcohol challenges as well as in early withdrawal states is well established

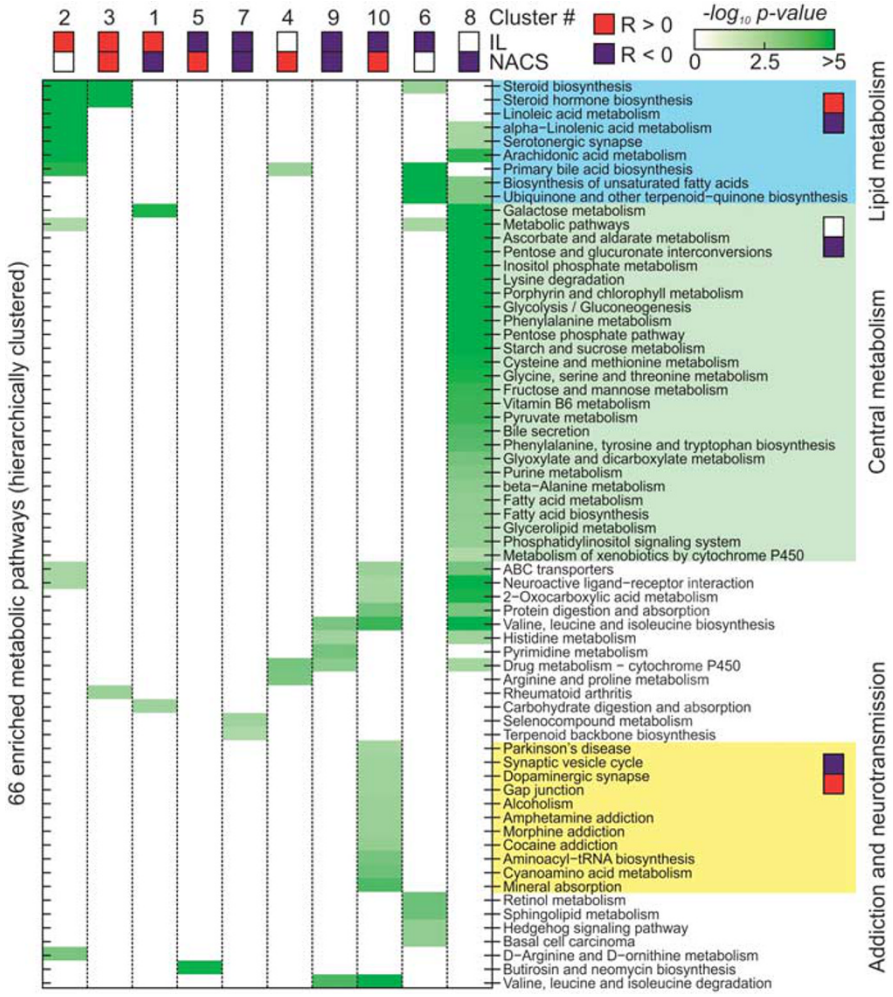

Figure 3 Metabolic pathway enrichment analysis of significantly correlating metabolites. The metabolic pathway enrichment analysis was performed for each correlation cluster shown in Figure 2b. The clusters and direction of correlation by color coding are represented at the top. A total of 66 pathways were significantly ($p<0.05$, hypergeometric test) enriched in at least one cluster. Green shading indicates the *p*-value. Pathways are sorted by hierarchical clustering based on the Euclidean distances of enrichment *p*-values, and groups of pathways with similar correlation patterns are classified according to broader biological function. A consensus correlation pattern representing the average of all involved cluster for each of these three broad function categories is shown within every block of biological functions. Three groups of altered biological functions were observed, namely lipid metabolism, central energy metabolism, as well as addiction and neurotransmission.

(Di Chiara, 1995; Weiss *et al*, 1996; Koob, 2013). Although alcohol administration or intake is accompanied by increased accumbal dopamine release, acute withdrawal typically results in a hypodopaminergic state. However, these previous data typically show a normalization of extracellular dopamine levels within 3 days. Here we assessed tissue concentration of dopamine that cannot be compared with extracellular dopamine levels measured by *in vivo* microdialysis. Furthermore, under the present conditions of voluntarily consumed alcohol, no acute withdrawal reaction is expected. Nevertheless, our data support a pivotal role of dopaminergic neurotransmission in excessive alcohol consumption of postdependent rats as high dopamine levels last at least for 3 days of abstinence. In addition, enkephalins have been shown to mediate alcohol intake (George *et al*, 1991) and Met-enkephalin levels increase after acute alcohol challenge (Marinelli *et al*, 2005). Furthermore, we found robust correlation of Met-enkephalin with dopamine levels in the nucleus accumbens shell. Together, the data provide further support for a functional role for dopamine–opiate systems interaction in the effects of alcohol (Björk *et al*, 2013).

Impairments in executive control and the disruption of the subcortical reward circuitry are known risk factors for drug addiction (Everitt and Robbins, 2005; Goldstein and Volkow, 2011; Kasanetz *et al*, 2012). Here, we found opposing patterns of metabolite correlations with alcohol drinking in infralimbic cortex and accumbens shell. This neurometabolic fingerprint might be an indicator of disturbed prefrontocortical functions. The depletion of metabolites in the infralimbic cortex of high alcohol-drinking rats as seen in our data could ultimately lead to typical behaviors seen in subjects with damage to the ventromedial prefrontal cortex such as socially inappropriate behavior, impulsivity, and poor judgment (Bechara *et al*, 1994; Urcelay and Dalley, 2011). Moreover, the divergent correlation pattern of the infralimbic (negative) and accumbens shell (positive) is intriguing, as we could

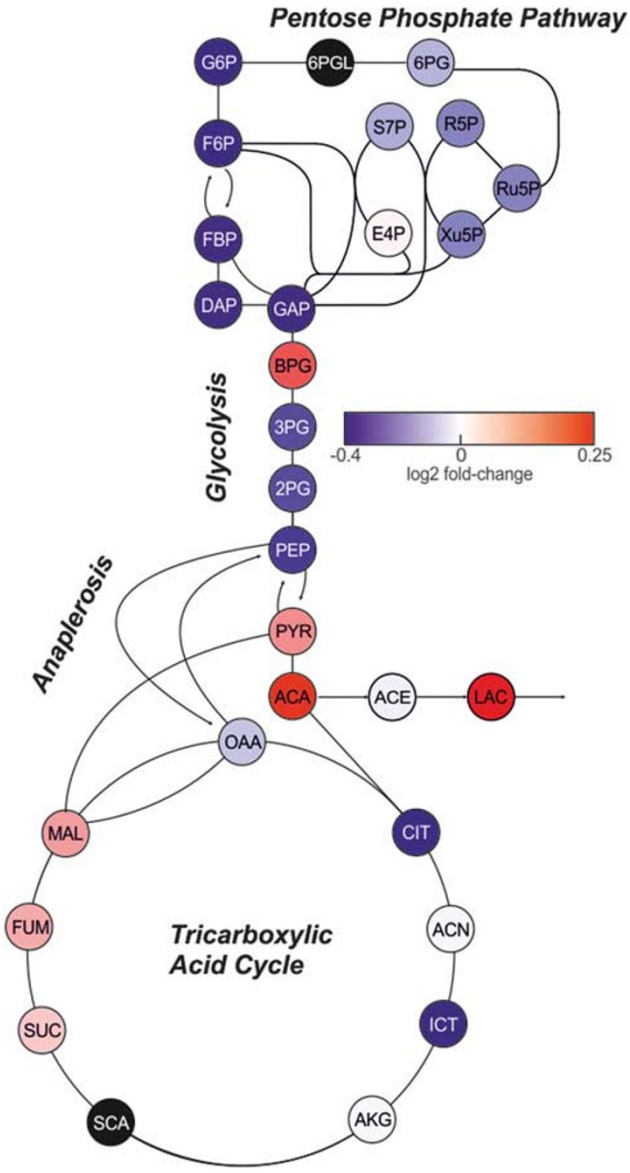

Figure 4 Elevated consumption results in decreased glycolysis and PPP metabolite levels specifically in the nucleus accumbens shell. Metabolite fold changes between animals with normal and elevated alcohol consumption are shown by color shading. Positive values indicate an accumulation and negative values a depletion of metabolite pools in animals with elevated consumption. Metabolites represented by solid black circles were not detected. G6P, glucose 6-phosphate; 6PGL, 6-phosphogluconolactone; 6PG, 6-phosphogluconate; F6P, fructose 6-phosphate; S7P, sedoheptulose 7-phosphate; R5P, ribose 5-phosphate; Ru5P, ribulose 5-phosphate; Xu5P, xylulose 5-phosphate; E4P, erythrose 4-phosphate; FBP, fructose 1,6-bisphosphate; DAP, dihydroxyacetone phosphate; GAP, glyceraldehyde 3-phosphate; BPG, 1,3-bisphosphoglycerate; 3PG, 3-phosphoglycerate; 2PG, 2-phosphoglycerate; PEP, phosphoenolpyruvate; PYR, pyruvate; LAC, lactate; ACA, acetyl-CoA; ACE, acetate; OAA, oxaloacetate; CIT, citrate, ACN, *cis*-aconiate; ICT, isocitrate; AKG, 2-oxoglutarate; SCA, succinyl-CoA; SUC, succinate; FUM, fumarate; MAL, malate.

previously show a loss of inhibitory control in the infralimbic cortex (Meinhardt *et al*, 2013) that may result in increased activity in the accumbens shell. In turn, this may lead to high energy demands in the shell that could underlie the observed alterations in energy metabolism in the shell. Deficits in energy metabolism have also been reported for morphine addiction (Chen *et al*, 2007; Yang *et al*, 2007; Deng *et al*, 2012). Alternatively, alcohol at relevant pharmacological doses is known to shift substrate utilization in the brain away from glucose toward acetate oxidation (Volkow *et al*, 2006, 2013; Wang *et al*, 2013). However, these changes were observed after an acute alcohol challenge and are thus difficult to compare with the present observations from 3-day abstinent rats. Nevertheless, such metabolic flexibility appears to be more pronounced in heavy drinkers compared with light drinkers (Jiang *et al*, 2013), and seems to be also a genetic trait in rodent lines bred for high alcohol consumption (Björk *et al*, 2006; Sommer *et al*, 2006; Zimatkin *et al*, 2011). Together, these data provide further evidence that energy metabolism and ultimately mitochondrial function in distinct brain regions such as the nucleus accumbens shell may be highly relevant components for the development of addictive disorders.

In conclusion, we have demonstrated the feasibility of detecting brain states related to alcohol consumption by analyzing neurometabolomic signatures. The data point toward profound alterations within the infralimbic–accumbens shell pathway, with mitochondrial dysregulation in the accumbens shell emerging as a so far underappreciated pathophysiological mechanism in the development of alcoholism. From a clinical perspective, metabolic positron emission tomography can identify metabolic alterations in distinct brain regions: whether or not such altered responses could comprise a biomarker for assessing the pathophysiology of alcohol addiction in clinical populations remains to be studied.

FUNDING AND DISCLOSURE

The authors declare no conflict of interest.

ACKNOWLEDGEMENTS

We thank Elisabeth Röbel for assistance in laboratory experiments. Funding was obtained by the Bundesministerium für Bildung und Forschung within the frameworks of ERA-Net TRANSALC (FKZ01EW1112) and eMeds (BMBF 01ZX1311A (Spanagel *et al*, 2013), and by Deutsche Forschungsgemeinschaft center grant SFB636).

REFERENCES

Alexander-Kaufman K, Harper C (2009). Transketolase: observations in alcohol-related brain damage research. *Int J Biochem Cell Biol* **41**: 717–720.

Arlinde C, Sommer W, Björk K, Reimers M, Hyytiä P, Kiianmaa K *et al* (2004). A cluster of differentially expressed signal transduction genes identified by microarray analysis in a rat genetic model of alcoholism. *Pharmacogenomics J* **4**: 208–218.

Ayanwuyi LO, Carvajal F, Lerma-Cabrera JM, Domi E, Björk K, Ubaldi M *et al* (2013). Role of a genetic polymorphism in the corticotropin-releasing factor receptor 1 gene in alcohol drinking and seeking behaviors of marchigian sardinian alcohol-preferring rats. *Front Psychiatry* **4**: 23.

Bechara A, Damasio AR, Damasio H, Anderson SW (1994). Insensitivity to future consequences following damage to human prefrontal cortex. *Cognition* **50**: 7–15.

Björk K, Hansson AC, Sommer WH (2010). Genetic variation and brain gene expression in rodent models of alcoholism implications for medication development. *Int Rev Neurobiol* **91**: 129–171.

Björk K, Saarikoski ST, Arlinde C, Kovanen L, Osei-Hyiaman D, Ubaldi M *et al* (2006). Glutathione-S-transferase expression in the brain: possible role in ethanol preference and longevity. *FASEB J* **20**: 1826–1835.

Björk K, Tronci V, Thorsell A, Tanda G, Hirth N, Heilig M *et al* (2013). β-Arrestin 2 knockout mice exhibit sensitized dopamine release and increased reward in response to a low dose of alcohol. *Psychopharmacology (Berl)* **230**: 439–449.

Bogdanov M, Matson WR, Wang L, Matson T, Saunders-Pullman R, Bressman SS *et al* (2008). Metabolomic profiling to develop blood biomarkers for Parkinson's disease. *Brain* **131**: 389–396.

Chen X-L, Lu G, Gong Y-X, Zhao L-C, Chen J, Chi Z-Q *et al* (2007). Expression changes of hippocampal energy metabolism enzymes contribute to behavioural abnormalities during chronic morphine treatment. *Cell Res* **17**: 689–700.

Deng Y, Bu Q, Hu Z, Deng P, Yan G, Duan J *et al* (2012). 1) H-nuclear magnetic resonance-based metabonomic analysis of brain in rhesus monkeys with morphine treatment and withdrawal intervention. *J Neurosci Res* **90**: 2154–2162.

Dettmer K, Aronov PA, Hammock BD (2007). Mass spectrometry-based metabolomics. *Mass Spectrom Rev* **26**: 51–78.

Di Chiara G (1995). The role of dopamine in drug abuse viewed from the perspective of its role in motivation. *Drug Alcohol Depend* **38**: 95–137.

Di Chiara G, Imperato A (1988). Drugs abused by humans preferentially increase synaptic dopamine concentrations in the mesolimbic system of freely moving rats. *Proc Natl Acad Sci USA* **85**: 5274–5278.

Everitt BJ, Robbins TW (2005). Neural systems of reinforcement for drug addiction: from actions to habits to compulsion. *Nat Neurosci* **8**: 1481–1489.

Fuhrer T, Heer D, Begemann B, Zamboni N (2011). High-throughput, accurate mass metabolome profiling of cellular extracts by flow injection-time-of-flight mass spectrometry. *Anal Chem* **83**: 7074–7080.

Gelernter J, Kranzler HR, Sherva R, Almasy L, Koesterer R, Smith AH *et al* (2014). Genome-wide association study of alcohol dependence: significant findings in African- and European-Americans including novel risk loci. *Mol Psychiatry* **19**: 41–49.

George SR, Roldan L, Lui A, Naranjo CA (1991). Endogenous opioids are involved in the genetically determined high preference for ethanol consumption. *Alcohol Clin Exp Res* **15**: 668–672.

Gika HG, Ji C, Theodoridis GA, Michopoulos F, Kaplowitz N, Wilson ID (2012). Investigation of chronic alcohol consumption in rodents via ultra-high-performance liquid chromatography-mass spectrometry based metabolite profiling. *J Chromatogr A* **1259**: 128–137.

Goldstein RZ, Volkow ND (2011). Dysfunction of the prefrontal cortex in addiction: neuroimaging findings and clinical implications. *Nat Rev Neurosci* **12**: 652–669.

Howland JG, Taepavarapruk P, Phillips AG (2002). Glutamate receptor-dependent modulation of dopamine efflux in the nucleus accumbens by basolateral, but not central, nucleus of the amygdala in rats. *J Neurosci* **22**: 1137–1145.

Imperato A, Di Chiara G (1986). Preferential stimulation of dopamine release in the nucleus accumbens of freely moving rats by ethanol. *J Pharmacol Exp Ther* **239**: 219–228.

Jiang L, Gulanski BI, De Feyter HM, Weinzimer SA, Pittman B, Guidone E *et al* (2013). Increased brain uptake and oxidation of acetate in heavy drinkers. *J Clin Invest* **123**: 1605–1614.

Kaddurah-Daouk R, Krishnan KRR (2009). Metabolomics: a global biochemical approach to the study of central nervous system diseases. *Neuropsychopharmacology* **34**: 173–186.

Kanehisa M (2002). The KEGG database. *Novartis Found Symp* **247**: 91–101, discussion 101–103, 119–128, 244–252.

Kasanetz F, Lafourcade M, Deroche-Gamonet V, Revest J-M, Berson N, Balado E *et al* (2012). Prefrontal synaptic markers of cocaine addiction-like behavior in rats. *Mol Psychiatry* **18**: 729–737.

Koob GF (2013). Theoretical frameworks and mechanistic aspects of alcohol addiction: alcohol addiction as a reward deficit disorder. *Curr Top Behav Neurosci* **13**: 3–30.

Koob GF, Volkow ND (2010). Neurocircuitry of addiction. *Neuropsychopharmacology* **35**: 217–238.

Liu J, Lewohl JM, Harris RA, Iyer VR, Dodd PR, Randall PK *et al* (2006). Patterns of gene expression in the frontal cortex discriminate alcoholic from nonalcoholic individuals. *Neuropsychopharmacology* **31**: 1574–1582.

Macey DJ, Schulteis G, Heinrichs SC, Koob GF (1996). Time-dependent quantifiable withdrawal from ethanol in the rat: effect of method of dependence induction. *Alcohol* **13**: 163–170.

Marinelli PW, Bai L, Quirion R, Gianoulakis C (2005). A microdialysis profile of Met-enkephalin release in the rat nucleus accumbens following alcohol administration. *Alcohol Clin Exp Res* **29**: 1821–1828.

Masuo Y, Imai T, Shibato J, Hirano M, Jones OA, Maguire ML *et al* (2009). Omic analyses unravels global molecular changes in the brain and liver of a rat model for chronic Sake (Japanese alcoholic beverage) intake. *Electrophoresis* **30**: 1259–1275.

Mayfield RD, Lewohl JM, Dodd PR, Herlihy A, Liu J, Harris RA (2002). Patterns of gene expression are altered in the frontal and motor cortices of human alcoholics. *J Neurochem* **81**: 802–813.

Meinhardt MW, Sommer WH (2014). The postdependent state in rats as a model for medication development in alcoholism. *Addict Biol* (doi:10.1111/adb.12187; e-pub ahead of print).

Meinhardt MW, Hansson AC, Perreau-Lenz S, Bauder-Wenz C, Stählin O, Heilig M *et al* (2013). Rescue of infralimbic mGluR2 deficit restores control over drug-seeking behavior in alcohol dependence. *J Neurosci* **33**: 2794–2806.

Noori HR, Spanagel R, Hansson AC (2012). Neurocircuitry for modeling drug effects. *Addict Biol* **17**: 827–864.

Parsons MP, Li S, Kirouac GJ (2007). Functional and anatomical connection between the paraventricular nucleus of the thalamus and dopamine fibers of the nucleus accumbens. *J Comp Neurol* **500**: 1050–1063.

Pasikanti KK, Ho PC, Chan ECY (2008). Gas chromatography/mass spectrometry in metabolic profiling of biological fluids. *J Chromatogr B Analyt Technol Biomed Life Sci* **871**: 202–211.

Patti GJ, Yanes O, Siuzdak G (2012). Innovation: metabolomics: the apogee of the omics trilogy. *Nat Rev Mol Cell Biol* **13**: 263–269.

Paxinos G, Watson C (1998). *The Rat Brian in Stereotaxic Coordinates*. Academic Press: San Diego.

Pontieri FE, Tanda G, Di Chiara G (1995). Intravenous cocaine, morphine, and amphetamine preferentially increase extracellular dopamine in the "shell" as compared with the "core" of the rat nucleus accumbens. *Proc Natl Acad Sci USA* **92**: 12304–12308.

Rehm J, Mathers C, Popova S, Thavorncharoensap M, Teerawattananon Y, Patra J (2009). Global burden of disease and injury and economic cost attributable to alcohol use and alcohol-use disorders. *Lancet* **373**: 2223–2233.

Reimers M, Heilig M, Sommer WH (2005). Gene discovery in neuropharmacological and behavioral studies using Affymetrix microarray data. *Methods* **37**: 219–228.

Rimondini R, Arlinde C, Sommer W, Heilig M (2002). Long-lasting increase in voluntary ethanol consumption and transcriptional regulation in the rat brain after intermittent exposure to alcohol. *FASEB J* **16**: 27–35.

Rimondini R, Sommer W, Heilig M (2003). A temporal threshold for induction of persistent alcohol preference: behavioral evidence in a rat model of intermittent intoxication. *J Stud Alcohol* **64**: 445–449.

Sévin DC, Sauer U (2014). Ubiquinone accumulation improves osmotic-stress tolerance in Escherichia coli. *Nat Chem Biol* **10**: 266–272.

Sommer W, Arlinde C, Heilig M (2005). The search for candidate genes of alcoholism: evidence from expression profiling studies. *Addict Biol* **10**: 71–79.

Sommer W, Hyytiä P, Kiianmaa K (2006). The alcohol-preferring AA and alcohol-avoiding ANA rats: neurobiology of the regulation of alcohol drinking. *Addict Biol* **11**: 289–309.

Sommer WH, Rimondini R, Hansson AC, Hipskind PA, Gehlert DR, Barr CS *et al* (2008). Upregulation of voluntary alcohol intake, behavioral sensitivity to stress, and amygdala crhr1 expression following a history of dependence. *Biol Psychiatry* **63**: 139–145.

Spanagel R (2009). Alcoholism: a systems approach from molecular physiology to addictive behavior. *Physiol Rev* **89**: 649–705.

Spanagel R, Durstewitz D, Hansson A, Heinz A, Kiefer F, Köhr G *et al* (2013). A systems medicine research approach for studying alcohol addiction. *Addict Biol* **18**: 883–896.

Storey JD, Tibshirani R (2003). Statistical significance for genome-wide studies. *Proc Natl Acad Sci USA* **100**: 9440–9445.

Treutlein J, Kissling C, Frank J, Wiemann S, Dong L, Depner M *et al* (2006). Genetic association of the human corticotropin releasing hormone receptor 1 (CRHR1) with binge drinking and alcohol intake patterns in two independent samples. *Mol Psychiatry* **11**: 594–602.

Urcelay GP, Dalley JW (2011). Linking ADHD, impulsivity, and drug abuse: a neuropsychological perspective. *Curr Top Behav Neurosci* **9**: 173–197.

Volkow ND, Kim SW, Wang G-J, Alexoff D, Logan J, Muench L *et al* (2013). Acute alcohol intoxication decreases glucose metabolism but increases acetate uptake in the human brain. *Neuroimage* **64**: 277–283.

Volkow ND, Wang G-J, Franceschi D, Fowler JS, Thanos PPK, Maynard L *et al* (2006). Low doses of alcohol substantially decrease glucose metabolism in the human brain. *Neuroimage* **29**: 295–301.

Wang J, Du H, Jiang L, Ma X, de Graaf RA, Behar KL *et al* (2013). Oxidation of ethanol in the rat brain and effects associated with chronic ethanol exposure. *Proc Natl Acad Sci USA* **110**: 14444–14449.

Weiss F, Parsons LH, Schulteis G, Hyytiä P, Lorang MT, Bloom FE *et al* (1996). Ethanol self-administration restores withdrawal-associated deficiencies in accumbal dopamine and 5-hydroxytryptamine release in dependent rats. *J Neurosci* **16**: 3474–3485.

Yang L, Sun ZS, Zhu Y (2007). Proteomic analysis of rat prefrontal cortex in three phases of morphine-induced conditioned place preference. *J Proteome Res* **6**: 2239–2247.

Yao JK, Reddy RD (2005). Metabolic investigation in psychiatric disorders. *Mol Neurobiol* **31**: 193–203.

Zaitsu K, Miyawaki I, Bando K, Horie H, Shima N, Katagi M *et al* (2013). Metabolic profiling of urine and blood plasma in rat models of drug addiction on the basis of morphine, methamphetamine, and cocaine-induced conditioned place preference. *Anal Bioanal Chem* **406**: 1339–1354.

Zhou Z, Karlsson C, Liang T, Xiong W, Kimura M, Tapocik JD *et al* (2013). Loss of metabotropic glutamate receptor 2 escalates alcohol consumption. *Proc Natl Acad Sci USA* **110**: 16963–16968.

Zimatkin SM, Oganesian NA, Kiselevski YV, Deitrich RA (2011). Acetate-dependent mechanisms of inborn tolerance to ethanol. *Alcohol Alcohol* **46**: 233–238.

Supplementary Information accompanies the paper on the Neuropsychopharmacology website (http://www.nature.com/npp)